表2　疫学研究と介入研究の差

	介入研究（RCT）	疫学研究
評価対象	精製標品（薬剤）	複合品（食品），ライフスタイル
期間	短期（数カ月―数年）	長期（数十年）
対象	疾病患者	コホート （一般地域住民のことが多い）
評価基準	疾病の進行抑制，治癒	疾病発症頻度の抑制

い．認知症を発症した患者を同質な2群に分け，有効と思われる成分を投与された群と偽薬（プラセボ）を与えられた群で症状の進行を比較する（randomized controlled study = RCT）（表2）．

これまでの研究では，疫学研究では野菜摂取の抗認知症効果を示す多くの結果が報告されている[6,7]一方，介入研究のほとんどは失敗に終わっている[8]．この原因は，食品由来成分は薬剤のような強力な作用をもたないため，短期的な治療効果というより長期的な予防効果を検討するための研究デザインが必要なためではないかと考えられる．

野菜由来の微量成分の抗認知症作用のメカニズム

■抗酸化作用

アルツハイマー病などの老年性認知症の最大のリスクファクターは老化である．“老化のフリーラジカル説”[9]は広く受け入れられている概念ではあるが，その実態はなんであろうか．酸化ストレスにより生体を構成する分子，たとえば核酸，蛋白質，脂質などが酸化修飾を受け，構造変化をきたしたり，機能不全を起こす．とくに，脳神経のような分裂能力の乏しい細胞ではこのような酸化修飾分子を新しい細胞をつくること（再生）により排除できないため異常な構造をもつ分子が蓄積しやすい．たとえばアルツハイマー病の原因にかかわるAβの蓄積には脳内の酸化修飾分子の蓄積や，酸化ストレスの亢進が関与している可能性がある．ビタミンC，E，ポリフェノール類は抗酸化作用をもち，抗老化，抗老年病効果をもつと期待されているが，介入研究，とくにサプリメントの摂取が有効であったとの証明はなされていない．

■遺伝子発現制御作用

近年，食品由来成分，とくにポリフェノール類であるレスベラトロール[10]，カテキン[11]などが遺伝子の発現を制御し，老化，老年病を抑制することが報告され，注目を集めている．レスベラトロールは赤ワインに含まれ，昔から“フレンチパラドックス（フランス人はアルコール摂取量が多いのに動脈硬化性疾患が少ない）”の原因ではないかとされてきた．レスベラトロールの働きとして抗酸化作用のほかに，寿命遺伝子であるsirtuin familyを活性化することが報告され，さらに実験動物で寿命を延長させたり，インスリン耐性を増強したりすることが見出された．しかし，ヒトに対する長寿作用は確認されておらず，さらに，日本人はアルコール耐性が低いのでワインの多量摂取によるアルコール毒性の危険が高いため勧められない．

一般患者への指導はどうあるべきか

現在，科学的に実証された“認知症を防ぐ食生活”は存在しない．しかしながら疫学的研究，動物実験ともに適正な量の野菜の摂取が認知症予防に有効である可能性を示唆している．また，とくに認知症患者さんのなかには偏った食生活

を続けており，他からの指導，介入が必要な方がおられることも事実である．このような患者さんに対し，規則正しい食生活と適切な量の野菜の摂取を促すことは，摂取食品そのものの改善に加え，生活習慣全般の改善により認知症の予防あるいは進行防止につながる可能性がある．

おわりに

医食同源とは日本古来からの哲学であり，超高齢化社会を迎えた現在，予防医療，統合医療の重要性が高まっている．認知症を予防する食生活を科学的に検証することが今後の課題である．

文献

1) St George-Hyslop PH, Westaway DA. Alzheimer's disease. Antibody clears senile plaques. Nature 1999 ; 400 : 116-7.
2) Garcia-Alloza M, Borrelli LA, Rozkalne A, et al. Curcumin labels amyloid pathology in vivo, disrupts existing plaques, and partially restores distorted neurites in an Alzheimer mouse model. J Neurochem 2007 ; 102(4) : 1095-104.
3) Marambaud P, Zhao H, Davies P. Resveratrol promotes clearance of Alzheimer's disease amyloid-beta peptides. J Biol Chem 2005 ; 280(45) : 37377-82.
4) Rezai-Zadeh K, Shytle D, Sun N, et al. Green tea epigallocatechin-3-gallate (EGCG) modulates amyloid precursor protein cleavage and reduces cerebral amyloidosis in Alzheimer transgenic mice. J Neurosci 2005 ; 25(38) : 8807-14.
5) Ono K, Yoshiike Y, Takashima A, et al. Potent anti-amyloidogenic and fibril-destabilizing effects of polyphenols in vitro : implications for the prevention and therapeutics of Alzheimer's disease. J Neurochem 2003 ; 87(1) : 172-81.
6) Barberger-Gateau P, Raffaitin C, Letenneur L, et al. Dietary patterns and risk of dementia : the Three-City cohort study. Neurology 2007 ; 69(20) : 1921-30.
7) Dai Q, Borenstein AR, Wu Y, Jackson JC, Larson EB. Fruit and vegetable juices and Alzheimer's disease : the Kame Project. Am J Med 2006 ; 119(9) : 751-9.
8) Kreijkamp-Kaspers S, Kok L, Grobbee DE, et al. Effect of soy protein containing isoflavones on cognitive function, bone mineral density, and plasma lipids in postmenopausal women : a randomized controlled trial. JAMA 2004 ; 292(1) : 65-74.
9) Harman D. Aging : a theory based on free radical and radiation chemistry. J Gerontol 1956 ; 11(3) : 298-300.
10) Baur JA, Pearson KJ, Price NL. Resveratrol improves health and survival of mice on a high-calorie diet. Nature 2006 ; 444(7117) : 337-42.
11) Reznichenko L, Amit T, Youdim MB, Mandel S. Green tea polyphenol (-)-epigallocatechin-3-gallate induces neurorescue of long-term serum-deprived PC 12 cells and promotes neurite outgrowth. J Neurochem 2005 ; 93(5) : 1157-67.

*　　*　　*

砂糖(甘い菓子類)摂取の影響

自治医科大学附属さいたま医療センター　神経内科
大塚美恵子　*Otsuka, Mieko*

keyword
アルツハイマー病，高インスリン血症，
インスリン抵抗性，砂糖，菓子類

はじめに

2型糖尿病（T2DM）は世界的に急速に増加しており，全体的な運動不足と肥満の蔓延が拍車をかけている．T2DMはもはや中高年のたんなる疾患ではなく若年層においても現在，将来の健康を脅かす深刻な疾患とみなされている[1]．多くの疫学調査でT2DMはアルツハイマー病（AD）の発症と関連があるとされており[2,3,4]，さらに最近糖尿病をともなわない高インスリン血症も危険因子として注目されている[5]．

本稿では，AD患者の耐糖能異常と高インスリン血症の実態，食行動のなかでも砂糖（甘い菓子類）摂取との関連について調査した結果を中心に述べてゆく．

インスリンとアルツハイマー病に関する知見

インスリン受容体は脳に広く分布しており，とくに海馬に集中している．また，Frolichらの報告[6]ではAD患者の脳内インスリン受容体濃度が健常対照者に比較して増加している．これはインスリンシグナリングの欠乏を代償的に高めようとしているためと解釈されている．さらに，インスリン分解酵素Insulin-degrading enzyme（IDE）はアミロイドベータ蛋白（Aβ）の分解と除去に関連があり[7]，IDEはインスリンとの親和性が強いため高濃度のインスリンはIDEによるAβの分解を抑制し[7]，神経原線維を構成する重要な要素の一つであるタウ蛋白（τ）のリン酸化を増すとも報告されている．このようにインスリン調節異常はAβ沈着やτのリン酸化を増す[8]ことでAD発症にかかわっていると考えられる．したがって，インスリンとインスリン抵抗性の研究は，T2DMとADの関連を解明するのに期待される分野とみなされている．

アルツハイマー病患者の栄養学的問題点

ADと栄養の問題は糖尿病やインスリンに関する問題以外に，現在のところ以下の点に絞られてきている．まず，野菜・果物の摂取はADを予防し，ビタミンE，ビタミンCなどの抗酸化ビタミンが注目されている[9]．つぎに，魚の摂取はADを予防し，魚油に含まれるドコサヘキサエン酸（DHA；22：6 n-3）やエイコサペンタエン酸（EPA；20：5 n-3）などのn-3系多価不飽和脂肪酸（PUFA）の役割が注目されている[10]．第3に動脈硬化の危険因子である高ホモシステイン血症がADでも認められ，ビタミンB_6，ビタミンB_{12}，葉酸の欠乏との関連が注目されている．これらは酸化ストレス，慢性炎症，血管

Radiat Med (2007) 25:255–262
DOI 10.1007/s11604-007-0132-8

ORIGINAL ARTICLE

Direct comparison study between FDG-PET and IMP-SPECT for diagnosing Alzheimer's disease using 3D-SSP analysis in the same patients

Takashi Nihashi · Hiroshi Yatsuya
Kazumasa Hayasaka · Rikio Kato · Shoji Kawatsu
Yutaka Arahata · Katsushige Iwai · Akinori Takeda
Yukihiko Washimi · Kumiko Yoshimura
Kanako Mizuno· Takashi Kato · Shinji Naganawa
Kengo Ito

Received: December 19, 2006 / Accepted: February 23, 2007

Abstract
Purpose. The purpose of this study was to evaluate and compare the diagnostic ability of 2-[^{18}F]-fluoro-2-deoxy-D-glucose (FDG) positron emission tomography (PET) and *N*-isopropyl-*p*-^{123}I iodoamphetamine single photon emission computed tomography (IMP-SPECT) using three-dimensional stereotactic surface projections (3D-SSP) in patients with moderate Alzheimer's disease (AD).

Materials and methods. FDG-PET and IMP-SPECT were performed within 3 months in 14 patients with probable moderate AD. Z-score maps of FDG-PET and IMP-SPECT images of a patient were obtained by comparison with data obtained from control subjects. Four expert physicians evaluated and graded the glucose hypometabolism and regional cerebral blood flow (rCBF), focusing in particular on the posterior cingulate gyri/precunei and parietotemporal regions, and determined the reliability for AD. Receiver operating characteristic (ROC) curves were applied to the results for clarification. To evaluate the correlation between two modalities, the regions of interest (ROIs) were set in the posterior cingulate gyri/precunei and parietotemporal region on 3D-SSP images, and mean Z-values were calculated.

Conclusion. No significant difference was observed in the area under the ROC curve (AUC) between FDG-PET and IMP-SPECT images (FDG-PET 0.95, IMP-SPECT 0.94). However, a significant difference ($P < 0.05$) was observed in the AUC for the posterior cingulate gyri/precuneus (FDG-PET 0.94, IMP-SPECT 0.81). The sensitivity and specificity of each modality were 86%, and 97% for FDG-PET and 70% and 100% for IMP-SPECT. We could find no significant difference between FDG-PET and IMP-SPECT in terms of diagnosing moderate AD using 3D-SSP. There was a high correlation between the two modalities in the parietotemporal region (Spearman's $r = 0.82$, $P < 0.001$). The correlation in the posterior cingulate gyri/precunei region was lower than that in the parietotemporal region (Spearman's $r = 0.63$, $P < 0.016$).

T. Nihashi (✉) · K. Hayasaka · R. Kato
Department of Radiology, National Center for Geriatrics and Gerontology, 36-3 Gengo, Morioka-Cho, Ohbu 474-8522, Japan
Tel. +81-562-46-2311; Fax +81-562-48-2373
e-mail: dr284@hotmail.com

H. Yatsuya
Department of Pubic Health, Nagoya University School of Medicine, Nagoya, Japan

S. Kawatsu
Department of Radiology, Kyoritsu General Hospital, Nagoya, Japan

Y. Arahata · K. Iwai · A. Takeda · Y. Washimi
Department of Neurology, National Center for Geriatrics and Gerontology, Ohbu, Japan

K. Yoshimura · K. Mizuno · T. Kato · K. Ito
Department of Brain Science and Molecular Imaging, National Center for Geriatrics and Gerontology, Ohbu, Japan

S. Naganawa
Department of Radiology, Nagoya University Graduate School of Medicine, Nagoya, Japan

Key words 3D-SSP · Alzheimer's disease · SPECT · PET

Introduction

For the clinical diagnosis of Alzheimer's disease (AD), regional glucose metabolism and cerebral blood flow (rCBF) are measured by positron emission tomography (PET) and single photon emission computed tomography (SPECT), respectively. Several studies have reported that changes in the regional glucose metabolism or rCBF are useful for the diagnosis of AD.[1–8]

Recent computational advances have improved the detection of regional metabolic and perfusion change using three-dimensional stereotactic surface projections (3D-SSP) or statistical parametric mapping (SPM) for the clinical diagnosis.[9–16] These two methods use PET and SPECT to analyze an individual brain in comparison with a standard brain, after stereotactic normalization, pixel by pixel or voxel by voxel. Ishii et al. showed that the fully automatic diagnostic system, using 3D-SSP, was able to perform at a diagnostic level similar to that of the visual inspection of conventional axial images by experts using the glucose analog 2-[^{18}F]-fluoro-2-deoxy-D-glucose (FDG)-PET.[17] Imabayashi et al. showed that the ability of 3D-SSP to discriminate early AD patients from control subjects was superior to that of visual inspection.[14] Tang et al. reported that the addition of 3D-SSP to the transaxial section display of SPECT improved the reproducibility and the diagnostic performance of AD.[12]

In terms of a comparison between PET and SPECT, it is apparent that PET has the advantage of greater sensitivity and greater spatial resolution. SPECT is the most widely available modality for functional neuroimaging techniques to evaluate dementia. Because the availability of PET is limited, PET is not used as often as SPECT clinically. Recently, the use of 3D-SSP or SPM has enabled the diagnosis of AD with greater accuracy.

Few reports have made a direct comparison of the diagnostic ability between PET and SPECT using statistical brain mapping methods in the same patients. Therefore, the purpose of the present study is to compare the ability to discriminate an AD pattern from healthy subjects using a 3D-SSP analysis of FDG-PET and *N*-isopropyl-*p*-^{123}I iodoamphetamine (IMP)-SPECT with visual interpretation by four expert physicians.

Methods

Subjects

Informed consent was obtained from all subjects prior to their participation in this study, which was approved by the ethics committee at our institution. FDG-PET and IMP-SPECT were performed on 14 patients (6 men, 8 women) within at least 3 months. The mean age was 70.1 ± 8.5 years. These patients were diagnosed as having probable AD according to the National Institute of Neurological and Communicative Disorders and Stroke (NINCDS) and the Alzheimer's disease and Related Disorders Association (ADRDA) criteria. The mean score of the Mini-Mental State Examination (MMSE) for these patients was 18.8 ± 4.3. For the FDG-PET study, seven subjects (four men, three women; mean age 61.2 years) participated as normal controls (NC), and for the IMP-SPECT study, nine subjects (two men, seven women; mean age 70.1 years) participated as normal controls.

FDG-PET

An ECAT EXACT HR 47 PET camera (Siemens/CTI, Germany) was used, and imaging was performed using two-dimensional acquisition at 60 min after intravenous administration of ^{18}F-FDG (370 MBq). Before FDG-PET scanning, the subjects rested in a supine position with eyes closed in a quiet room. The collected data were reconstructed into 128 × 128 pixel image matrices. Tissue attenuation of annihilation photons was corrected by transmission scans using rotating ^{68}Ge/^{68}Ga line sources. The in-plane spatial resolution was 4.0 × 3.9 mm in full-width at half-maximum (FWHM). The patient fasted for at least 6 h prior to the examination. Normal glucose levels were confirmed prior to the PET scan.

IMP-SPECT

A total of 222 MBq (6 mCi) of ^{123}I-IMP (Nihon Mediphysics, Hyogo, Japan) was injected into an antecubital vein while the subjects rested in a supine position with eyes closed in a quiet room. A single blood sample was obtained from the brachial artery between 9 and 10 min after the ^{123}I-IMP administration. SPECT scanning was carried out between 15 and 45 minutes after injection using a two-head rotating GCA 7200DI gamma camera (Toshiba, Tokyo, Japan) fitted with low-energy, high-resolution collimators. The data were acquired in 128 × 128 matrices through a 18° rotation at an angle interval of 4°. The projection data were prefiltered through a Butterworth filter and reconstructed using a Ramp back-

Table 1. Normal database of FDG-PET and IMP-SPECT

Method	No.	Sex (M/F)	Age
FDG-PET	37	23/11	59.0
IMP-SPECT	18	7/F	69.9

FDG-PET, 2-[^{18}F]-fluoro-2-deoxy-D-glucose positron emission tomography; IMP-SPECT, *N*-isopropyl-*p*-^{123}I iodoamphetamine single photon emission computed tomography

projection filter. Chang's attenuation correction and scattering correction using the triple energy window method were applied to the reconstructed images. The in-plane spatial resolution was 11.1 mm in FWHM. The final image slices were set parallel to the orbitomeatal line and were obtained at an interval of 3.44 mm through the entire brain. The rCBF images were quantitated according to the IMP-ARG method.[18]

Statistical images (3D-SSP)

The original FDG-PET and IMP-SPECT data were analyzed by an iSSP (SSP; Nihon Mediphysics) program, which was modified based on the NEUROSTAT program (Dr. Minoshima, Department of Radiology and Bioengineering, University of Washington, Seattle, WA, USA). After rotation and centering of the data set, the original data were realigned to the bicommissural line (AC-PC) and transformed into a stereotactic standard Talairach space. The cortical peak activity was projected onto the brain surface, and the peak value was projected back and assigned to the originating surface pixel. The extracted data sets were displayed on eight different angles, including the lateral, medial, superior, inferior, anterior, and posterior views. With the 3D-SSP programs in NEUROSTAT, the pixel values were normalized to the whole brain, thalamus, pons, and cerebellum (Fig. 1). The pixel values of an individual's image were compared with a normal database that originated at our institution (Table 1). The normal database was built as follows: 18 normal subjects (7 men, 11 women; mean age 69.9 years) for IMP-SPECT and 37 normal subjects (23 men, 14 women; mean age 59.0 years) for FDG-PET.

Statistical analysis/visual interpretation

Four nuclear medicine physicians randomly interpreted FDG-PET images of 14 AD patients and 7 NCs and IMP-SPECT images of 9 NCs. The interpretation of each image was performed at separate sessions, respectively. The statistical analyses were conducted using the following procedure. Two areas of the brain, the posterior cingulate gyri/precunei and parietotemporal region in each image (which were determined as characteristic for AD in advance of the study) were evaluated.[9] The degree of reduction in glucose metabolism or rCBF were interpreted, and a score of 5 was assigned if the change was considered "apparent decrease," which is characteristic of AD. Accordingly, scores of 4 to 1 were assigned to the changes that were considered "probable decrease," "unclear," "probable not a decrease," and "apparently not a decrease," respectively. Then, the reliability was evaluated using five steps similar to the regional evaluation.

When laterality was observed in a visual interpretation, the evaluation of a regional change was performed as follows. The scores assigned to the right and left sides (of the brain) of FDG-PET were compared for each side of the brain, and the higher score was recorded as the case's FDG-PET score for the specific area of the brain. The side of the higher FDG-PET score was considered a regional finding, and the IMP-SPECT score of the same side was recorded as the case's IMP-SPECT score. If the right- and left-side FDG-PET scores were the same, the higher score in IMP-SPECT was recorded as the regional finding. In fact, there were no discrepancies between the FDG-PET scores and the IMP-SPECT images in terms of laterality.

Second, the ratings of four readers were pooled for each area and for each image. The ROC analysis was performed for the graphics presentation, and the area under the curve was calculated to express the diagnostic accuracy of each image and each area numerically. Confidence intervals (CIs) of the AUC were used to test the difference in overall diagnostic accuracy between the images, the upper and lower limits of which were calculated either by adding or subtracting the standard error of the AUC times 1.96 for 95% CI and 1.65 for 90% CI. Because our primary interest lies in the difference in the diagnostic ability of FDG-PET from IMP-SPECT, we did not compare the difference in the AUC between the areas of the brain and did not take multiplicity in comparison into account. $P < 0.05$ was considered statistically significant. The statistical analyses were conducted using SPSS for Windows.

Correlation between FDG-PET and IMP-SPECT

To assess the agreement between two modalities, ROIs were set in the posterior cingulate gyri/precunei and parietotemporal region on 3D-SSP images, of which the pixel values were normalized to the whole brain bilaterally (Fig. 2). Then the mean Z-values of the right and left hemisphere were summed and used for analysis. We calculated kappa (κ) statistics, the proportion of concordance, and the Spearman's correlation coefficients of

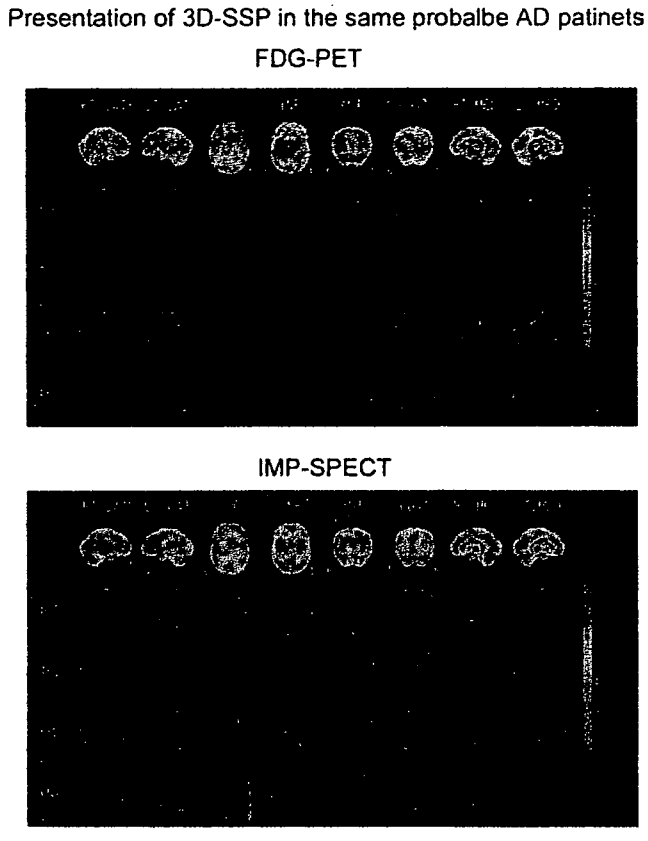

Fig. 1. Z-score images of three-dimensional stereotactic surface projections (3D-SSP) are shown from a representative Alzheimer's disease (AD) patient. These images demonstrate a decrease in the glucose metabolism and regional cerebral blood flow (rCBF). *Upper panel*: 2-[^{18}F]-Fluoro-2-deoxy-D-glucose positron emission tomography (FDG-PET). *Lower panel*: *N*-Isopropyl-*p*-^{123}I iodoamphetamine single photon emission computed tomography (IMP-SPECT). The extracted data sets are displayed on eight different angles, including the lateral (*RT LAT*, *LT LAT*), medial (*RT MED*, *LT MED*), superior (*SUP*), inferior (*INF*), anterior (*ANT*), and posterior (*POST*) views. With the 3D-SSP programs in NEUROSTAT, the pixel values are normalized to the whole brain (*GLB*), thalamus (*THL*), cerebellum (*CBL*), and pons (*PNS*)

Z-values in each area (the posterior cingulate gyri/precunei and parietotemporal region). For assessing κ statistics and the proportion of concordance, Z-values were first categorized according to their quartiles. Then the lowest quartile was considered as the "decrease" category. The κ statistic is defined as the agreement beyond chance divided by the amount of agreement possible by chance. As in most studies, $\kappa > 0.75$ was taken to represent excellent agreement beyond chance, 0.40–0.75 to mean fair agreement, and <0.40 to mean poor agreement.[19]

Results

Figure 3 shows the results of the clinical diagnosis of AD by 3D-SSP. The AUC of FDG-PET was 0.952 ± 0.023, and that of IMP-SPECT was 0.935 ± 0.026. There was no significant difference between FDG-PET and IMP-SPECT. Table 2 shows the results of each interpreter and the sum as the diagnosis ability. The sensitivity and specificity of each modality were 86%, and 97% for FDG-PET and 70%, and 100% for IMP-SPECT, respectively (Table 3).

Table 2. Results of visual inspection of 3D-SSP by each interpreter

	FDG-PET		IMP-SPECT	
Interpreter	AUC	SE	AUC	SE
A	0.939	0.057	0.976	0.026
B	0.954	0.047	0.96	0.041
C	0.888	0.074	0.821	0.091
D	0.995	0.01	1	0
Sum	0.952	0.023	0.935	0.026

3D-SSP, three-dimensional stereotactic surface projections; AUC, area under the curve; SE, standard error

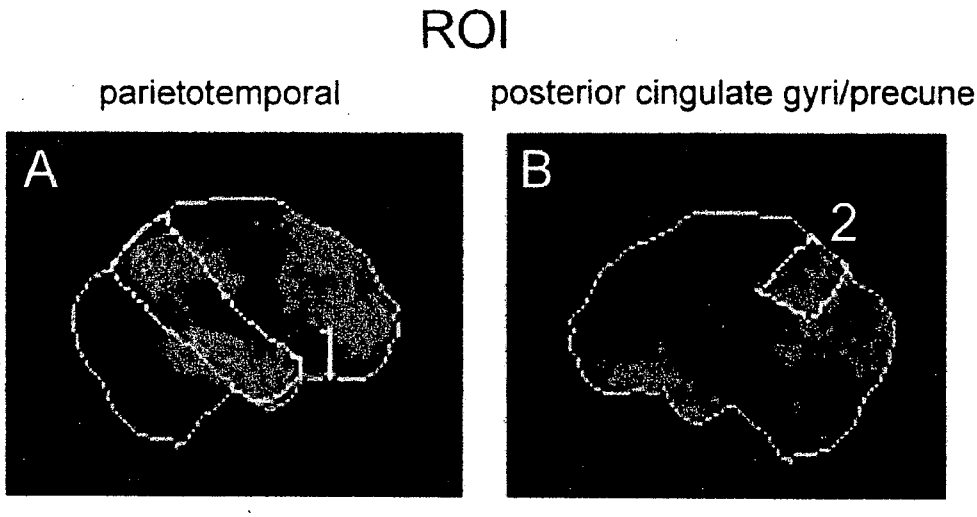

Fig. 2. Regions of interest (ROI) were set in the posterior cingulate gyri/precunei (B) and parietotemporal region (A) on 3D-SSP images of FDG-PET, in which the pixel values were normalized to the whole brain bilaterally

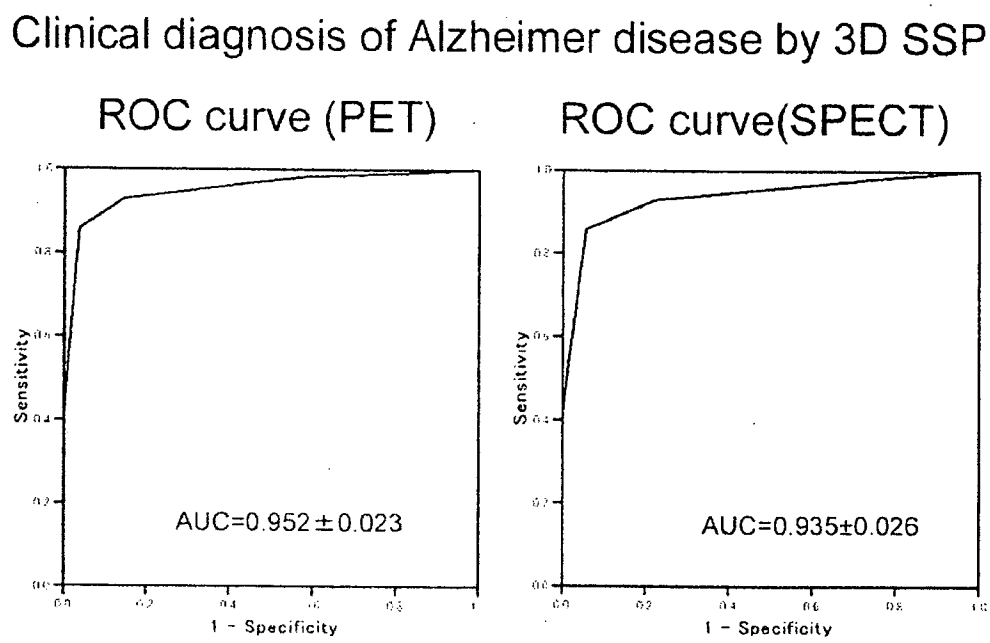

Fig. 3. Receiver operating characteristic (ROC) curves for clinical diagnosis of AD with visual inspection by experts. There was no significant difference between PET and SPECT. *AUC*, area under the curve

Table 3. Results of visual inspection of 3D-SSP by each interpreter: sensitivity and specificity

Interpreter	FDG-PET		IMP-SPECT	
	Sensitivity (%)	Specificity (%)	Sensitivity (%)	Specificity (%)
A	93	100	64	100
B	79	100	79	100
C	86	86	64	100
D	86	100	71	100
Sum	344	386	278	400
Average	86	97	70	100

Figure 4 shows the regional evaluation of the posterior cingulate gyri/precuneus and the parietotemporal region. The AUC of FDG-PET was 0.935 ± 0.028, and that of IMP-SPECT was 0.807 ± 0.046 in the posterior cingulate gyri/precuneus. A significant difference between FDG-PET and IMP-SPECT was observed ($P < 0.05$). The AUC of FDG-PET was 0.871 ± 0.038, and that of IMP-SPECT was 0.802 ± 0.046 in the parietotemporal region. There was no significant difference between FDG-PET and IMP-SPECT detected for this region.

Interrater agreement among four nuclear medicine physicians was evaluated by intraclass correlation coefficient with the Spearman-Brown correction. For both PET and SPECT, the agreement in the ratings among four raters were high: PET 0.94, SPECT 0.96.

There was a high correlation of Z-values between FDG-PET and IMP-SPECT in the parietotemporal region (Spearman's $r = 0.82$, $P < 0.001$). The correlation of the two modalities in the posterior cingulate gyri/precunei region was lower than that in the parietotemporal region (Spearman's $r = 0.63$, $P < 0.016$). In terms of the proportion of concordance and κ statistics, there was a perfect agreement in the parietotemporal region (both 1.0, $P < 0.001$). The proportion of concordance in the posterior cingulate gyri/precunei region was comparable (0.71), but agreement beyond chance evaluated by the κ statistics was poor and not significantly greater than zero (0.15, $P = 0.57$).

Discussion

Voxel-based statistical mapping methods, such as 3D-SSP and SPM, have been reported to be useful when delineating AD individuals from normal subjects.[9–16,20,21] Honda et al showed that 3D-SSP enhanced the specificity of SPECT inspection by nuclear medicine physicians

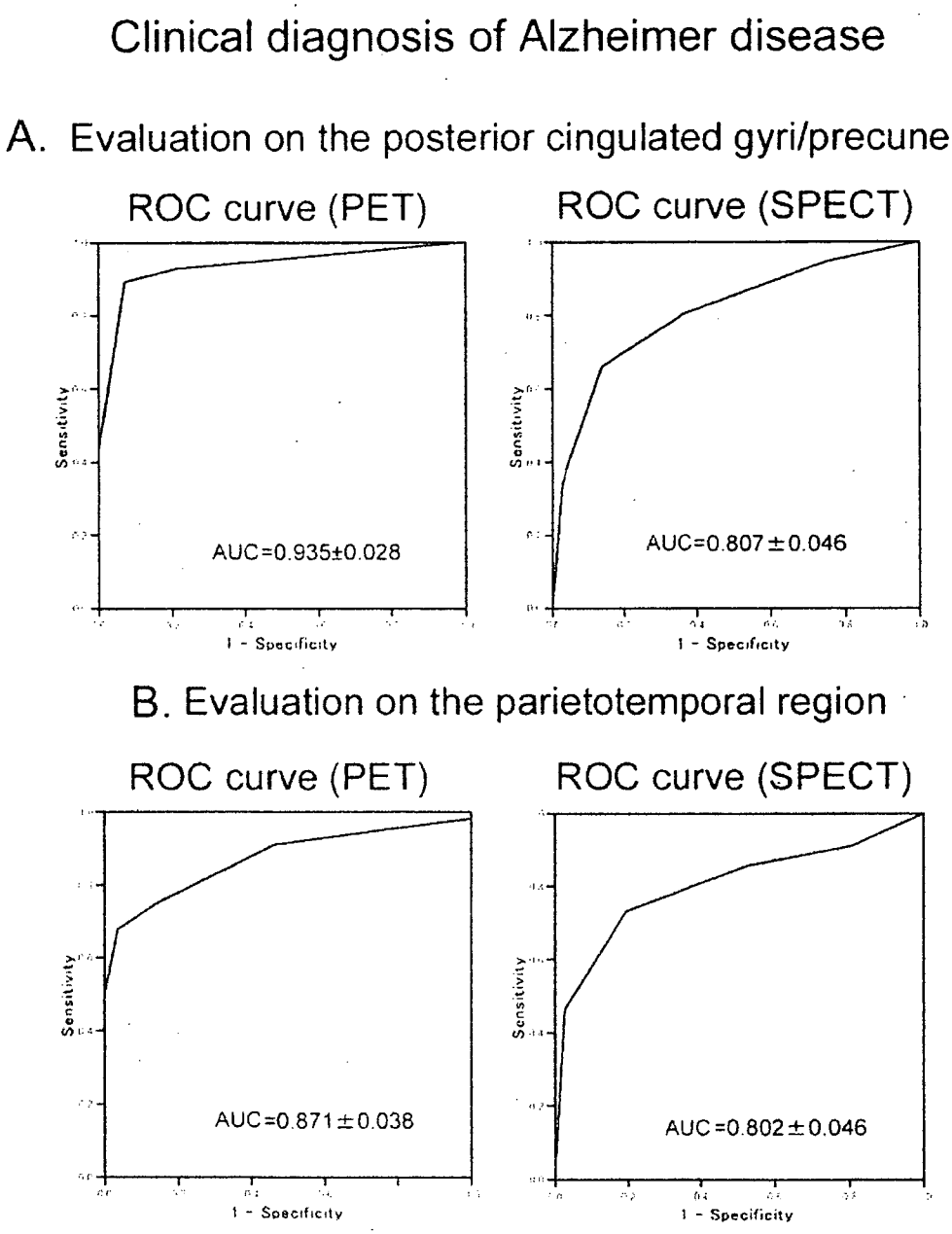

Fig. 4. ROCs for clinical diagnosis of AD with visual inspection of the posterior cingulated gyri/precuneus (**A**) and the parietotemporal region (**B**). For evaluation of the posterior cingulated gyri/precuneus, PET is significantly superior to SPECT

and the performance of the automated diagnosis, when focusing on the posterior cingulate gyri and precunei, exceeded that of the physicians when evaluating SPECT with and without 3D-SSP.[11] These reports showed that voxel-based statistical mapping methods may add useful information when diagnosing AD. The usefulness of such statistical methods has become clear, and these methods are used frequently clinically.

A few studies have compared FDG-PET and rCBF SPECT directly in terms of diagnosing AD. Mielke et al. reported that both PET and SPECT are able to distinguish AD patients from controls. On the other hand, for differentiation between AD and vascular dementia (VD), PET was shown to be superior to SPECT.[22] Messa et al. reported that both PET and SPECT were able to detect characteristic temporoparietal abnormalities in probable AD, whereas for the evaluation for other associative areas PET was superior to SPECT.[23] Silverman reported that higher diagnostic accuracy was obtained with PET than with SPECT, and the increased accuracy was estimated to be approximately 15%–20%.[24] Herholz et al. reported that correspondence between PET and SPECT was limited to the main finding of temporoparietal and posterior cingulate functional impairment in mild to moderate AD using SPM.[25] Although many studies have shown that PET is superior to SPECT in terms of diag-

nosing AD, it seems that a decisive difference has not been determined concerning the diagnostic ability of PET and SPECT as far as the posterior cingulate gyri/precuneus and the parietotemporal region are concerned, which are the characteristic regions for AD.

In the present study, our purpose was to compare directly the diagnostic ability of FDG-PET and IMP-SPECT using 3D-SSP and focusing on as the posterior cingulate gyri/precuneus and the parietotemporal region. Our results show that there was no significant difference between FDG-PET and IMP-SPECT in terms of diagnosing AD using 3D-SSP. However, there was a tendency that FDG-PET was slightly superior to IMP-SPECT, especially when evaluating the posterior cingulate gyri/precuneus. These results are consistent with those of previous studies and our clinical experience. We considered two possibilities to explain the findings. First, a possible reason why FDG-PET is superior to IMP-SPECT is that the metabolic change due to degeneration might slightly proceed to a decrease in rCBF. Second, PET has the advantage of greater sensitivity and greater spatial resolution. Both possibilities were plausible.

We found that there was a high correlation of Z-values between FDG-PET and IMP-SPECT in the parietotemporal region; in contrast, there was not a good correlation in the posterior cingulate gyri/precunei region. These results showed that there was the difference between the glucose metabolic and rCBF changes in the posterior cingulate gyri/precunei region. We considered two possibilities regarding this problem. First, coupling the glucose metabolic change and rCBF change might depend on the degree of the degeneration. Therefore, in the posterior cingulate gyri/precunei region, because the degenerative change is slight, the change in glucose metabolism might be greater than that of the rCBF change. Second, distributions of the glucose metabolism and rCBF were not the same in every area of the brain. Sakamoto and Ishii showed that there are great glucose metabolic and rCBF differences between the medial temporal lobe, the cerebellum, and other brain regions in the normal human brain.[26] If there was a difference between the glucose metabolism and rCBF in the posterior cingulate gyri/precunei region, it was not impossible to understand this result. To evaluate the finding in the posterior cingulate gyri/precunei region, further studies are needed from a radiological and/or pathological approach.

There are three restrictions to the present study. First, the normal controls and normal database differed, respectively, for FDG-PET and IMP-SPECT. Ideally, for each examination, the normal controls and database should be the same. However, prescribing nuclear medicine to healthy subjects twice in a short time is difficult. Second, in the present study, we analyzed only moderately affected AD patients. Recently, Dobert et al. evaluated the diagnostic potential of FDG-PET and SPECT in terms of early detection and the differential diagnosis of early dementia in the same patients and showed that PET was the superior imaging method, especially for detecting early AD or mixed-type dementia.[27] If we analyze early or mild AD, the results may change. Third, owing to a relatively small number of subjects, the statistical power might have been limited in the present study. In an illustrative example dataset where a total of about 160 subjects were studied in which the correlation of the underlying bivariate binormal distribution is 0.75, statistical power to detect a 0.10 difference in the AUC of the two modalities was estimated as 0.75.[28] In the present study, a total of about 90 subjects were studied where the AUC difference of more than 0.1 had been expected, and the statistical power of the analysis would have been retained to a similar degree. Thus, the present finding of no difference could be interpreted as relevant. Ideally, further studies with larger sample sizes are needed to examine whether these two modalities are really equivalent in diagnosing AD given that we did not observe a statistically significant difference in the AUC between FDG-PET and IMP-SPECT.

Using 3D-SSP, our results show that FDG-PET and IMP-SPECT have similar diagnostic ability in moderately affected AD patients. However, there was the tendency that the ability of FDG-PET to detect probable AD was superior to that of IMP-SPECT. Specifically, for regional glucose metabolism or cerebral blood flow analysis of the posterior cingulate gyri/precuneus, PET was significantly superior to SPECT.

References

1. Duara R, Grady C, Haxby J, Sundaram M, Cutler NR, Heston L, Moore A, et al. Positron emission tomography in Alzheimer's disease. Neurology 1986;3:879–87.
2. Heiss WD, Szelies B, Kessler J, Herholz K. Abnormalities of energy metabolism in Alzheimer's disease studied with PET. Ann N Y Acad Sci 1991;640:65–71.
3. Silverman DH, Small GW, Chang CY, Lu CS, Kung De Aburto MA, Chen W, et al. Positron emission tomography in evaluation of dementia: regional brain metabolism and long-term outcome. JAMA 2001;286:2120–7.
4. Bradley KM, O'Sullivan VT, Soper ND, Nagy Z, King EM, Smith AD, et al. Cerebral perfusion SPECT correlated with Braak pathological stage in Alzheimer's disease. Brain 2002; 125:1772–81.
5. Ishii K. Clinical application of positron emission tomography for diagnosis of dementia. Ann Nucl Med 2002;16:515–25.
6. Herholz K, Salmon E, Perani D, Baron JC, Holthoff V, Frolich L, et al. Discrimination between Alzheimer dementia and controls by automated analysis of multicenter FDG PET. Neuroimage 2002;17:302–16.

7. Herholz K. PET studies in dementia. Ann Nucl Med 2003;17: 79–89.
8. Hirao K, Ohnishi T, Hirata Y, Yamashita F, Mori T, Moriguchi Y, et al. The prediction of rapid conversion to Alzheimer's disease in mild cognitive impairment using regional cerebral blood flow SPECT. Neuroimage 2005; 28:1014–21.
9. Minoshima S, Frey KA, Koeppe RA, Foster NL, Kuhl DE. A diagnostic approach in Alzheimer's disease using three-dimensional stereotactic surface projections of fluorine-18-FDG PET. J Nucl Med 1995;36:1238–48.
10. Burdette JH, Minoshima S, Vander Borght T, Tran DD, Kuhl DE. Alzheimer disease: improved visual interpretation of PET images by using three-dimensional stereotaxic surface projections. Radiology 1996;198:837–43.
11. Honda N, Machida K, Matsumoto T, Matsuda H, Imabayashi E, Hashimoto J, et al. Three-dimensional stereotactic surface projection of brain perfusion SPECT improves diagnosis of Alzheimer's disease. Ann Nucl Med 2003;17: 641–8.
12. Tang BN, Minoshima S, George J, Robert A, Swine C, Laloux P, et al. Diagnosis of suspected Alzheimer's disease is improved by automated analysis of regional cerebral blood flow. Eur J Nucl Med Mol Imaging 2004;31:1487–94.
13. Kaneko K, Kuwabara Y, Sasaki M, Ogomori K, Ichimiya A, Koga H, et al. Posterior cingulate hypoperfusion in Alzheimer's disease, senile dementia of Alzheimer type, and other dementias evaluated by three-dimensional stereotactic surface projections using Tc-99m HMPAO SPECT. Clin Nucl Med 2004;29:362–6.
14. Imabayashi E, Matsuda H, Asada T, Ohnishi T, Sakamoto S, Nakano S, et al. Superiority of 3-dimensional stereotactic surface projection analysis over visual inspection in discrimination of patients with very early Alzheimer's disease from controls using brain perfusion SPECT. J Nucl Med 2004; 45:1450–7.
15. Kemp PM, Hoffmann SA, Holmes C, Bolt L, Ward T, Holmes RB, et al. The contribution of statistical parametric mapping in the assessment of precuneal and medial temporal lobe perfusion by ^{99m}Tc-HMPAO SPECT in mild Alzheimer's and Lewy body dementia. Nucl Med Commun 2005;26: 1099–106.
16. Kim EJ, Cho SS, Jeong Y, Park KC, Kang SJ, Kang E, et al. Glucose metabolism in early onset versus late onset Alzheimer's disease: an SPM analysis of 120 patients. Brain 2005;128:1790–801.
17. Ishii K, Kono AK, Sasaki H, Miyamoto N, Fukuda T, Sakamoto S, et al. Fully automatic diagnostic system for early- and late-onset mild Alzheimer's disease using FDG PET and 3D-SSP. Eur J Nucl Med Mol Imaging 2006;10:1–9.
18. Iida H, Itoh H, Nakazawa M, Hatazawa J, Nishimura H, Onishi Y, et al. Quantitative mapping of regional cerebral blood flow using iodine-123-IMP and SPECT. J Nucl Med 1994;35:2019–30.
19. Fleiss J. The measurement of interrater agreement. In: Statistical methods for rates and proportions. 2nd edition. New York: Wiley; 1981. p. 212–36.
20. Dougall NJ, Bruggink S, Ebmeier KP. Systematic review of the diagnostic accuracy of ^{99m}Tc-HMPAO-SPECT in dementia. Am J Geriatr Psychiatry 2004;12:554–70.
21. Huang C, Wahlund LO, Almkvist O, Elehu D, Svensson L, Jonsson T, et al. Voxel- and VOI-based analysis of SPECT CBF in relation to clinical and psychological heterogeneity of mild cognitive impairment. Neuroimage 2003;19:1137–44.
22. Mielke R, Pietrzyk U, Jacobs A, Fink GR, Ichimiya A, Kessler J, et al. HMPAO SPET and FDG PET in Alzheimer's disease and vascular dementia: comparison of perfusion and metabolic pattern. Eur J Nucl Med 1994;21:1052–60.
23. Messa C, Perani D, Lucignani G, Zenorini A, Zito F, Rizzo G, et al. High-resolution technetium-99m-HMPAO SPECT in patients with probable Alzheimer's disease: comparison with fluorine-18-FDG PET. J Nucl Med 1994;35:210–6.
24. Silverman DH. Brain ^{18}F-FDG PET in the diagnosis of neurodegenerative dementias: comparison with perfusion SPECT and with clinical evaluations lacking nuclear imaging. J Nucl Med 2004;45:594–607.
25. Herholz K, Schopphoff H, Schmidt M, Mielke R, Eschner W, Scheidhauer K, et al. Direct comparison of spatially normalized PET and SPECT scans in Alzheimer's disease. J Nucl Med 2002;43:21–6.
26. Sakamoto S, Ishii K. Low cerebral glucose extraction rates in the human medial temporal cortex and cerebellum. J Neurol Sci 2000;172:41–8.
27. Dobert N, Pantel J, Frolich L, Hamscho N, Menzel C, Grunwald F. Diagnostic value of FDG-PET and HMPAO-SPET in patients with mild dementia and mild cognitive impairment: metabolic index and perfusion index. Dement Geriatr Cogn Disord 2005;20:63–70.
28. Zhou XH, Obuchowski NA, McClish DK. Statistical methods in diagnostic medicine. New York: Wiley; 2002.

日本臨牀　第65巻・第2号（平成19年2月号）別刷

特集：分子イメージング

パーキンソン病

新畑　豊　　加藤隆司　　伊藤健吾

臨床応用　脳の分子イメージング

パーキンソン病

新畑　豊[1]　加藤隆司[2]　伊藤健吾[2]

Molecular imaging in Parkinson's disease

[1]Yutaka Arahata, [2]Takashi Kato, [2]Kengo Ito
[1]Department of Neurology, [2]Department of Brain Science and Molecular Imaging,
National Center for Geriatrics and Gerontology

Abstract

Molecular imaging techniques using PET or SPECT have provided major insights into not only objective diagnosis of Parkinson's disease (PD), but also understanding the pathophysiological process in the disease progression. At disease onset, a compensatory hyperactivity of dopa decarboxylase in the nigrostriatal and extrastriatal dopaminergic pathways and upregulation of postsynaptic D2 receptor have been demonstrated. In the advanced stage, an excessively earlier release of dopamine from the residual neurons has been shown, suggesting a relationship with motor complications. In terms of therapy of PD, functional images have provided some objective evidences for possible neuroprotective effect of dopamine agonists, survival of fetal dopaminergic tissue grafted into patient's putamen, an increase of dopamine release by BDNF focal infusion therapy, and functional modification by deep brain stimulation. *In vivo* imaging of gene expression under developing may be informative in the future gene therapy in PD.

Key words: Parkinson's disease, positron emission tomography, single photon emission computed tomography, molecular imaging

はじめに

パーキンソン病(PD)の臨床的検査所見としては，X線CT，MRIなどでとらえられる脳の形態には特異的な変化は乏しい．実際に臨床症状を引き起こしている背景にある神経伝達物質や受容体などの様々な生化学的，機能的変化は，従来は死後脳においてのみ解析可能な課題であった．しかしながら，PET，SPECTなどの核医学的手法を用いた分子イメージングにより，これらの異常を生体において疾患の種々のステージでとらえることが可能となり，病態の解析や治療の評価が進められてきた．

本稿では，これらの核医学的手法を用いた脳機能イメージングによるPDに関する知見を紹介する．

1. PDの病態とドパミン神経の機能評価法

PDの臨床症状を引き起こす病態機序の中心

[1]国立長寿医療センター神経内科　[2]同長寿脳科学研究部

0047-1852/07/¥40/頁/JCLS

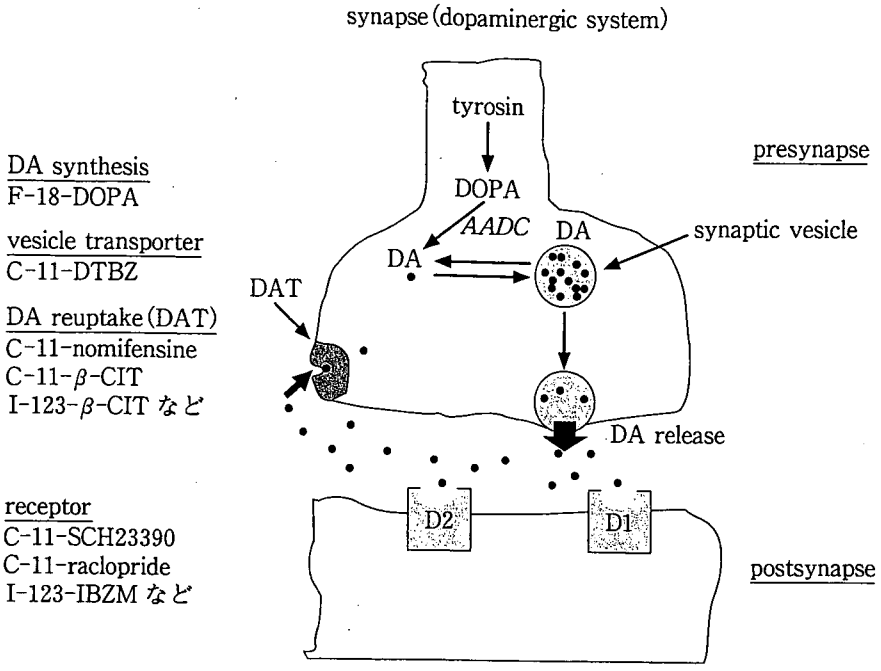

図1 ドパミン神経のシナプスの模式図と対応する標識薬剤
ドパミン(DA)の合成，再取り込み，受容体のそれぞれの機能を評価するPETおよびSPECT用の標識薬剤が開発されている．

となるのは，中脳黒質のドパミン神経脱落によるドパミン神経系の伝達障害にある．ドパミン神経系の分子イメージングによる評価法としては，ドパミンを放出する黒質-線条体神経を中心とするドパミン神経終末シナプス前部機能の評価とシナプス後部のレセプターの評価に大別される．シナプス前部の評価としては^{18}F-6-fluoro-dopa(FDOPA)を用いたPETが多くの研究に用いられているが，シナプス前部のドパミン再取り込み部位であるドパミントランスポーター(DAT)イメージングがPET，SPECTを用いて，また，シナプス小胞モノアミントランスポーター(VMAT2)のイメージングがPETを用いて行われており，それぞれの特徴が明らかとされてきた．

FDOPAは投与後，L-dopaと同様に脳血液関門を通過しドパミン神経に取り込まれ，芳香族アミノ酸脱炭酸酵素(AADC)により代謝を受け，^{18}F-6-fluoro-dopamineに転換され，その神経終末に蓄積される．これを用いたPETによるFDOPAの取り込み率は神経終末密度そのものではなくAADCの活性を反映すると考えられている．AADCはモノアミン神経に共通にみられる酵素であり，ドパミン系以外にもノルエピネフリン，セロトニン活性を反映する可能性がある．一方，細胞質で合成されたドパミンをはじめとするモノアミンはシナプス小胞に貯蔵されシナプス間隙への放出に備えられる．VMAT2を描出するリガンドである^{11}C-dihydrotetrabenazine(DTBZ)は，ドパミン，ノルエピネフリン，セロトニン，ヒスタミン終末を反映し得るが，線条体では95％以上がドパミン終末を反映する．シナプス間隙に放出されたドパミンはDATによりドパミン神経終末に再取り込みを受け，その伝達作用が終了する(図1)．

a. 早期PDにおけるドパミン系の代償機転

FDOPAは，黒質線条体ドパミンニューロンの投射先である線条体部分に最も高い集積がみられる．PDでは黒質の外側より神経細胞脱落が始まるが，FDOPAを用いたPETではこの病理所見を反映し，初期では被殻の後外側より取り込み低下がみられるようになり，経過とともに線条体の前方に向け低下が進行する．Yahr I

度のヘミパーキンソニズムの症例でも無症状の側に対応する線条体を含めて両側性に線条体でFDOPAの取り込み低下が明らかとなる[1]．早期のPDでは被殻のFDOPA取り込みの低下よりDATの低下が強くみられるが，進行期のPDでは両者の低下は同程度である[2]．これはPD病初期において残存するドパミン神経のAADC活性すなわちドパミン合成の代償的亢進を示すものと考えられ，FDOPAはPD初期では神経変性を過小評価する可能性がある[2]．臨床的な運動症状との相関はFDOPAがより高いが，残存神経終末密度の指標としては，DATがより正しく反映するものと考えられている[3]．PD病初期においてAADC活性の亢進がみられることは黒質-線条体以外にも中脳-辺縁系ドパミン神経系にも生じ，セロトニン神経系が代償的に活動している可能性がある[4]．更には，FDOPAと^{11}C-DTBZによるVMAT2，^{11}C-methylphenidateによるDATを同一患者で測定し比較した結果より，DATの低下はVMAT2の低下より強く，シナプス間隙でのドパミン濃度低下を代償するためDATは代償的に低下している可能性も指摘された．この結果より神経終末密度はVMAT2がDATより更に正確に反映する可能性がある[5]．

一方，ドパミン神経節後部の変化としては，未治療のPDにおいては，D_2 receptorの結合能の代償的亢進が特に被殻においてみられることが，^{11}C-raclopride PETにおいて示される[6]．これらのドパミン神経節前および後部の代償機転は早期あるいは未治療のPDにみられ，進行期では消失する．

b. 進行期のPDと運動合併症

進行期のPDにおける大きな問題点の一つとして，薬剤治療効果が不安定となりwearing-offやon-off現象，dyskinesiaなどの運動合併症の出現がある．進行期のPDにおいては，D_2 receptor結合能は正常化から低下する傾向がみられるが[6]，これは病態の進行に伴う可能性とともに，治療薬の影響による減少である可能性がある．raclopride はreceptorとの親和性が低く解離が起りやすいため，この特性を利用して内因性ドパミンの放出を測定することが可能である．運動合併症をもつ患者ではL-dopa投与後1時間でのシナプスドパミン濃度上昇が合併症をもたない患者よりも高く，4時間後には両群で差がみられないことより，peak-dose dyskinesiaの発症にドパミンのより早期の過剰な放出が関係している可能性があることが示されている[7]．

2. PDの治療効果の評価

a. ドパミンアゴニストの神経保護作用

L-dopaの長期投与による運動合併症誘発や実験レベルでの神経毒性などの観点より，ドパミンアゴニストでの治療開始が推奨されているが，臨床レベルで神経保護作用のエビデンスを提示するのは困難であった．このため，PET/SPECTによる2つの多施設共同臨床試験が行われた．REAL-PET study[8]はロピニロールとL-dopa投与群を2年間追跡し，その比較を^{18}F-FDOPAを用いて評価している．一方，CALM-PD/CIT study[9]では同様にプラミペキソールとL-dopaの単独投与群の比較を46カ月追跡照査し，^{123}I-β-CITを用いたDATの評価が行われた．この2つの研究いずれにおいてもドパミンアゴニストを用いた群ではL-dopa投与群に比して有意にドパミン神経のシナプス前機能の低下が抑制されていることが示された．薬剤による画像所見への修飾を排除できないなどの問題点はあるが，PDの初期治療をドパミンアゴニストで開始する一定の根拠を示した意義のある結果である．

b. 脳深部刺激療法(DBS)

DBSは脳深部に留置した電極に電気刺激を送り疾病の治療を行う方法であるが，PDにおいては主に視床下核(STN)および淡蒼球内節(GPi)刺激法が行われている．DBSは進行期の薬剤治療が困難な症例にも特にoff期症状改善に効果を上げるが，その作用機序は十分にわかっていない．PDではPETを用いた脳賦活検査においてjoystickなどの運動課題遂行時にレンズ核，前部帯状回，補足運動野，前頭前野の脳血流上昇が正常者より少ないことが知られてい

るが[10]，これらの脳賦活異常をDBSは抑制し，正常者に近い賦活が得られるようになる[11]．DBS刺激時，刺激停止時のraclopride の D_2 receptor占有率の差をみた検討より，DBSは直接的に内因性ドパミンの放出を促しているものではないことが明らかとされた[12]．

c. 移植治療

ヒト胎児黒質細胞をPD患者に移植する治療が欧米を中心に行われており，症状改善効果が得られている．Cochenらは移植後のDATとFDOPAの取り込みを調べ，DATの変化はないがFDOPAの取り込みは改善がみられることを示し，症状の改善はドパミン神経の再支配よりもAADC活性などの機能的改善が貢献しているものと推察している[13]．移植後のFDOPA取り込み改善は20カ月でプラトーに達するが，臨床症状はそれを超えて改善し，薬剤減量が可能となるとされる[14]．Piccini らは移植後10年を経過したPD患者において，グラフト側の被殻では正常のFDOPA集積がみられ，メタンフェタミン投与前後のraclopride を用いた内因性ドパミンの放出能の評価ではグラフト側で正常化していることを示した[15]．

d. 神経栄養因子による治療

GDNF(グリア細胞株由来神経栄養因子)はドパミン神経系に対し強い効果をもつ神経栄養因子で，マウスや霊長類におけるPDモデルにおいてドパミン神経の保護，再生が示されている．Gillらは5例のPD患者の被殻背側にカテーテル埋め込みGDNFを持続注入することにより，臨床症状の改善を確認するとともに，FDOPAの取り込みが改善することを示した[16]．これを受け，多施設共同での二重盲検試験が34人の中-高度PD患者に対し行われた．GDNF持続注入開始6カ月後にUPDRSの運動スコアの改善は10%でプラセボ群の4.5%に対して有意ではなかったが，FDOPAのKiは被殻後部で23.1%の上昇があり，プラセボ群の-8.8%に対し有意な改善がみられた[17]．

おわりに

このようにPET/SPECTによるドパミン神経機能をはじめとする脳機能の評価は，PDの病態解明とともに，新しい治療薬，治療法が開発される場合にヒトでの臨床応用の根拠ともなるべき客観的なエビデンスを提供でき，今後このような利用がより盛んになると思われる．移植医療における移植組織の入手の困難さから，PDにおいてもドパミン合成に必要な酵素遺伝子や神経栄養因子の遺伝子導入などの遺伝子治療が期待される．その場合には導入された遺伝子の発現を *in vivo* で確認することが求められるが，治療のための遺伝子導入と同時にこの発現確認のためのレポーター遺伝子を導入し，これにより発現する酵素あるいは受容体をPET/SPECTで画像化することで治療のための遺伝子の発現を確認することが可能である[18]．まだ動物実験の段階ではあるが，今後の発展が期待される．

■文　献

1) Ito K, et al: Statistical parametric mapping with ^{18}F-dopa PET shows bilaterally reduced striatal and nigral dopaminergic function in early Parkinson's disease. J Neurol Neurosurg Psychiatry **66**: 754-758, 1999.
2) Ribeiro MJ, et al: Dopaminergic function and dopamine transporter binding assessed with positron emission tomography in Parkinson disease. Arch Neurol **59**: 580-586, 2002.
3) Thobois S, et al: PET and SPECT functional imaging studies in Parkinsonian syndromes: From the lesion to its consequences. Neuroimage **23**: 1-16, 2004.
4) Whone AL, et al: Plasticity of the nigropallidal pathway in Parkinson's disease. Ann Neurol **53**: 206-213, 2003.
5) Lee CS, et al: In vivo positron emission tomographic evidence for compensatory changes in presynaptic dopaminergic nerve terminals in Parkinson's disease. Ann Neurol **47**: 493-503, 2000.

6) Dentresangle C, et al: Striatal D2 dopamine receptor status in Parkinson's disease: An ^{18}F-dopa and ^{11}C-Raclopride PET study. Mov Disord **14**: 1025-1030, 1999.
7) de la Fuente-Fernandez R, et al: Levodopa-induced changes in synaptic dopamine levels increase with progression of Parkinson's disease: implications for dyskinesias. Brain **127**: 2747-2754, 2004.
8) Whone AL, et al: Slower progression of Parkinson's disease with ropinirole versus levodopa: The REAL-PET study. Ann Neurol **54**: 93-101, 2003.
9) Parkinson Study Group: Dopamine transporter brain imaging to assess the effects of pramipexole vs levodopa on Parkinson disease progression. JAMA **287**: 1653-1661, 2002.
10) Playford ED, et al: Impaired mesial frontal and putamen activation in Parkinson's disease: A positron emission tomography study. Ann Neurol **32**: 151-161, 1992.
11) Strafella AP, et al: Cerebral blood flow changes induced by subthalamic stimulation in Parkinson's disease. Neurology **60**: 1039-1042, 2003.
12) Strafella AP, et al: Subthalamic deep brain stimulation does not induce striatal dopamine release in Parkinson's disease. Neuroreport **14**: 1287-1289, 2003.
13) Cochen V, et al: Transplantation in Parkinson's disease: PET changes correlate with the amount of grafted tissue. Mov Disord **18**: 928-932, 2003.
14) Brooks DJ: Positron emission tomography imaging of transplant function. NeuroRx **1**: 482-491, 2004.
15) Piccini P, et al: Dopamine release from nigral transplants visualized in vivo in a Parkinson's patient. Nat Neurosci **2**: 1137-1140, 1999.
16) Gill SS, et al: Direct brain infusion of glial cell line-derived neurotrophic factor in Parkinson disease. Nat Med **9**: 589-595, 2003.
17) Lang AE, et al: Randomized controlled trial of intraputamenal glial cell line-derived neurotrophic factor infusion in Parkinson disease. Ann Neurol **59**: 459-466, 2006.
18) Phelps ME: Positron emission tomography provides molecular imaging of biological processes. Proc Natl Acad Sci USA **97**: 9226-9233, 2000.

1. 脳神経
1-2. 核医学

加藤　隆司[1)]，伊藤　健吾[1)]，新畑　豊[2)]

国立長寿医療センター研究所　長寿脳科学研究部[1)]　国立長寿医療センター病院　神経内科[2)]

Neuroimaging, Nuclear Medicine

Takashi Kato, M.D.,[1)] Kengo Ito, M.D.,[1)] and Yutaka Arahata, M.D.[2)]

1) Department of Brain Sciences and Molecular Imaging, National Institute for Longevity Sciences, National Center for Geriatrics and Gerontology
2) Department of Neurology, National Hospital for Geriatric Medicine, National Center for Geriatrics and Gerontology

NICHIDOKU-IHO
Vol. 52 No. 4 22–31 (2007)

Summary

This chapter describes radionuclide imaging as it relates to neurodegenerative dementias like Alzheimer's disease (AD), idiopathic Parkinson's disease (PD), and normal aging, among the various diseases of the elderly. The role of neuroimaging with nuclear medicine is to detect changes in neural activities that are caused by these diseases. Such changes may be indirect phenomena, but the imaging of neural functions provides physicians with useful, objective information regarding pathophysiology in the brain.

Brain activities change with age, with the elderly showing decreased brain function in memory, execution, and attention.

Age-dependent reduction in the global mean of cerebral blood flow (CBF) has been reported in many studies that have used X-133 and O-15 labeled gas, the spatial resolution of which is low. Partial volume correction (PVC) is available through the segmentation of grey matter from high-resolution T1-weighted magnetic resonance imaging. Meltzer reported that age-related change disappeared after PVC. The relative distribution of CBF and glucose metabolism has been examined on a voxel-by-voxel basis in many studies. The areas negatively correlated with age are the anterior part of the brain, especially the dorsolateral and medial frontal areas, anterior cingulate cortices, frontolateral and perisylvian cortices, and basal ganglia. The areas positively correlated with age are the occipital lobe, temporal lobe, sensorimotor cortex, and primary visual cortex.

It is not easy to define "normal aging". Aged people tend to have the potential for diseases like cerebral ischemia caused by arteriosclerosis. Ischemia results in volume loss of the gray matter and CBF. The ApoE e4 gene is a risk factor for AD, and carriers of the ApoE e4 allel show CBF-like AD even at a relatively young age. Hypo-glucose metabolism in the posterior cingulate cortex is seen in 5% of normal people over 50 years of age. This Alzheimer-like CBF/metabolic pattern needs further investigation.

The neural substrate of these age-dependent changes may be explained in a limited way by neural transmission. Glucose metabolism is known to be modified by the age-related changes in dopaminergic and serotonergic functions.

AD shows reduced CBF/glucose metabolism in the parieto-temporal association cortices, precuneus, and posterior cingulate cortex, while CBF is preserved in the primary sensory-motor area, occipital lobe, basal ganglia, and thalamus. Early-onset AD has more severe hypometabolism in the bilateral parietal and posterior cingulate cortices and precuneus region than late-onset AD. Late-onset AD shows a tendency of hypometabolism in the limbic system and medial frontal area. The diversity of clinical responses to Donepezil therapy in patients with AD is associated with regional CBF changes, mainly in the frontal lobe. CBF/glucose metabolism may be a promising marker to assess the impact of AchEI therapy on the brain function of patients with AD.

Dementia with Lewy body (DLB) represents decreased CBF/glucose metabolism in the occipital lobe, parietotemporal

area, precuneus, and posterior cingulate cortex. The occipital lobe is a discriminating indicator for differentiating AD and DLB, but it is not perfect. Decreased dopaminergic activity is observed in the striatum and limbic system in DLB with [F-18] FDOPA PET.

Frontotemporal dementia (FTD) shows hypo-perfusion/metabolism in the frontal and temporal lobes with variations. Pick-type dementia shows a typical frontal lobar pattern, whereas in the other type the main area of decrease may depend on the clinical symptoms.

No distinguishing pattern of CBF/metabolism is observed in PD. Presynaptic dopaminergic terminals are affected, although the dopaminergic post-synapse is preserved.

はじめに

高齢者の神経疾患にはさまざまなものがあるが、本稿ではアルツハイマー病(Alzheimer's disease：AD)などの変性性認知症、神経変性疾患であるパーキンソン(idiopathic Parkinson's disease：PD)病を対象として担当する。また、健常の加齢性変化についても述べる。

核医学診断の役割は、疾患によって生じた脳の神経活動の変化を捉えて、鑑別診断や病態の解明を行うことにある。多くの場合は、疾患の病因そのものを捉えるのではなく、いわば間接的変化を捉えることになる。癌診断の場合とは異なり、画像だけで診断できることは少なく、患者の年齢、臨床症状など、他の情報があって初めて診断できる場合が多い。

しかし、臨床症状に基づく診断が神経疾患の診断の基本であることは確かであるが、神経兆候も神経病理学的変化からみれば間接的なものである。経時的にみれば確実に診断できても、ある一時の時間断面ではすべての症状が出そろうとは限らず、境界的な兆候を示す例もある。そのような場合に、脳内で生じている病態を視覚化できる検査は有用である。脳血流/糖代謝は、四捨五入的にいえば局所における神経活動に相関する。したがって、これらを画像化することは、神経活動を画像化することであると言い換えることができる。

本稿では、このような脳の機能変化を捉える比較的一般的な検査である脳血流SPECT(single photon emission computed tomography)、脳糖代謝PET(positron emission tomography)を中心に述べ、必要に応じて神経伝達などの他のイメージングについてもふれる。

脳血流/糖代謝の加齢性変化

脳機能は、発達と加齢のなかで変化している。新生児から成人へ、そして成人した後も若年から中年、高齢と年齢を重ねるに従い変化する。高齢者の脳機能は若年者と比較して、記憶機能、実行、注意などの機能が低下するが、これらに対応する神経変化が生じており、脳血流や灰白質体積に反映される。

1．全脳平均血流量、糖代謝率

全脳血流/糖代謝の絶対値は健常成人の個人間のばらつきが大きい。値にして30%程度のばらつきがある。

全脳平均血流量の加齢性変化をみた検討が多数ある。1980年代からX-133 CT、O-15標識ガスPETなどによって行われた検討の多くが、全脳平均血流量は加齢に応じて減少することを報告している。これらの検査法は分解能が低く、部分容積効果の影響を受けていることが指摘されていた。部分容積効果を評価する試みは早くからあったが[1]、T1強調MRI画像から灰白質を分割(segmentation)する方法が実用的なものになって以降、部分容積効果を補正して評価されるようになった。

Meltzerらの検討によると、19歳から76歳までの健常者を対象としてH_2O PETで測定した脳血流量が、部分容積効果を補正する前は加齢性の低下傾向が認められたが、部分容積効果の補正によりその加齢性変化は消失した。また、部分容積効果を補正すると年齢層間の差異も認められなくなったとしている[2]。

全脳平均糖代謝率の分布は、若年～中年者ではほぼ変わらないが、50～60歳を超えると、全体の分布は低い方へ変位し出し、そのまま高い値を示す個体はあるものの、高齢になるほど平均値は低下するともいう。

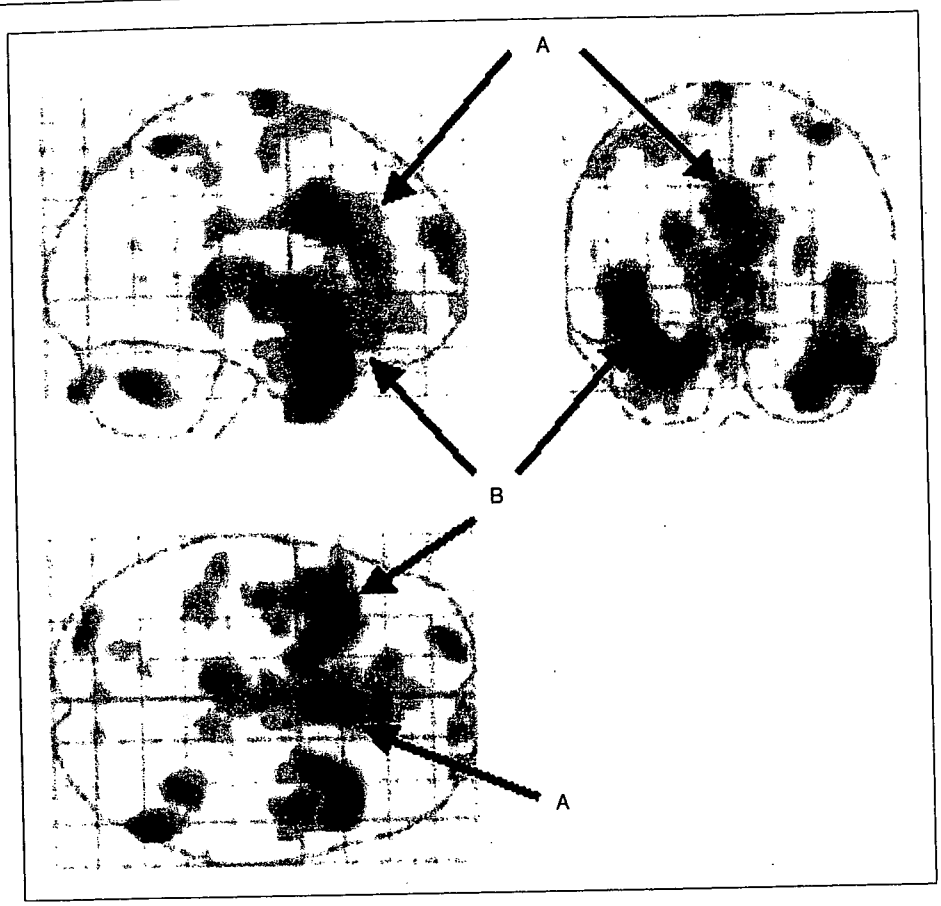

図1　脳糖代謝PET画像の健常の加齢性変化
健常の若年群に比べて健常の高齢群で糖代謝が低下している領域の3方向の投影表示($p < 0.01$, uncorrected)．前部帯状回(A)と傍シルビウス裂領域(B)で糖代謝の加齢性の低下が認められる．

2．脳血流 / 糖代謝の相対的分布

脳内の血流 / 糖代謝の相対的分布が、高齢者でどのように変化するかは、voxel-baseの統計解析により初めて詳細な検討が可能になった。いくつかの研究報告[3-6]があるが、次のようにまとめることができる。

年齢に相関して低下する領域は、前頭葉皮質の大半(特に背外側と内側)、前部帯状回、前外側傍シルビウス裂皮質、基底核である。この中で最も強い相関を示す傾向があるのは、前部帯状回である。基底核は、萎縮、脳室拡大が影響していると考えられている。逆に年齢に相関して上昇ないし、保たれる領域は、後頭葉、側頭葉、一次運動感覚野、一次視覚野である[2]。

脳血流 / 糖代謝は、灰白質体積の減少に起因する部分容積効果の影響を受けていると考えられる(図1)。加齢性変化の灰白質体積との関係について検討もなされている。Matsudaらは、部分容積効果の補正の有無にかかわらず、ECD(ethylcysteinate dimer)SPECT脳血流と年齢の負の相関が傍シルビウス裂領域や前頭葉領域にみられ、萎縮に起因しない真の加齢性変化の存在を示すものであると結論づけている[7]。他方、Yanaseらが、FDG PETで行った検討では、部分容積効果の補正を行うと、傍シルビウス裂、前頭葉、前部帯状回における年齢との負の相関が消えてしまうことから、脳糖代謝の変化は萎縮の効果をみたものであるとしている[5]。血流 / 糖代謝の結果が一致しない理由としては、局所の脳血流 / 糖代謝が解離するような何らかの病態生理が働いている、ECD、FDG各トレーサーの集積度が血流 / 糖代謝をそれぞれ忠実に反映していない、対象としている被検者の違いなどが可能性として考えられる。